



University of Dundee

Aerobic and anaerobic biosynthesis of nano-selenium for remediation of mercury contaminated soil

Wang, Xiaonan; Zhang, Daoyong; Pan, Xiangliang; Lee, Duu Jong; Al-Misned, Fahad A.; Mortuza, M. Golam; Gadd, Geoffrey Michael

Published in:
Chemosphere

DOI:
[10.1016/j.chemosphere.2016.12.020](https://doi.org/10.1016/j.chemosphere.2016.12.020)

Publication date:
2017

Document Version
Peer reviewed version

[Link to publication in Discovery Research Portal](#)

Citation for published version (APA):

Wang, X., Zhang, D., Pan, X., Lee, D. J., Al-Misned, F. A., Mortuza, M. G., & Gadd, G. M. (2017). Aerobic and anaerobic biosynthesis of nano-selenium for remediation of mercury contaminated soil. *Chemosphere*, 170, 266-273. DOI: [10.1016/j.chemosphere.2016.12.020](https://doi.org/10.1016/j.chemosphere.2016.12.020)

General rights

Copyright and moral rights for the publications made accessible in Discovery Research Portal are retained by the authors and/or other copyright owners and it is a condition of accessing publications that users recognise and abide by the legal requirements associated with these rights.

- Users may download and print one copy of any publication from Discovery Research Portal for the purpose of private study or research.
- You may not further distribute the material or use it for any profit-making activity or commercial gain.
- You may freely distribute the URL identifying the publication in the public portal.

Take down policy

If you believe that this document breaches copyright please contact us providing details, and we will remove access to the work immediately and investigate your claim.

1 **Aerobic and anaerobic biosynthesis of nano-selenium for remediation of mercury**
2 **contaminated soil**

3

4 Xiaonan Wang ^{a, c}, Geoffrey Michael Gadd ^{a, d}, Daoyong Zhang ^{a, e}, Xiangliang Pan ^{a, b, *}, Duu-Jong
5 Lee ^f, Fahad A. Al-Misned ^g, M. Golam Mortuza ^{g, h}

6

7 ^a *Xinjiang Key Laboratory of Environmental Pollution and Bioremediation, Xinjiang Institute of*
8 *Ecology and Geography, Chinese Academy of Sciences, Urumqi 830011, China*

9 ^b *College of Environment, Zhejiang University of Technology, Hangzhou 310014, China*

10 ^c *University of Chinese Academy of Sciences, Beijing 100049, China*

11 ^d *Geomicrobiology Group, School of Life Sciences, University of Dundee, Dundee DD1 5EH,*
12 *Scotland, UK*

13 ^e *State Key Laboratory of Environmental Geochemistry, Institute of Geochemistry, Chinese*
14 *Academy of Sciences, Guiyang, 550002, China*

15 ^f *Department of Chemical Engineering, National Taiwan University, Taipei 10617, Taiwan*

16 ^g *Department of Zoology, College of Science, King Saud University, Riyadh 11451, Saudi Arabia*

17 ^h *Department of Zoology, Faculty of Life and Earth Science, Rajshahi University, Rajshahi 6205,*
18 *Bangladesh*

19

20 *For correspondence. E-mail xiangliangpan@163.com ; Tel. +86 991 7885 446; Fax +86 991
21 7885 446.

22

23

24 © 2016. This manuscript version is made available under the CC-BY-NC-ND 4.0 license
25 <http://creativecommons.org/licenses/by-nc-nd/4.0/>

26 **Running title:** Biosynthesis of nano-Se⁰ and mercury remediation

27

28 **ABSTRACT**

29 Selenium (Se) nanoparticles are often synthesized by anaerobes. However, anaerobic
30 bacteria cannot be directly applied for bioremediation of contaminated top soil which
31 is generally aerobic. In this study, a selenite-reducing bacterium, *Citrobacter freundii*
32 Y9, demonstrated high selenite reducing power and produced elemental
33 nano-selenium nanoparticles (nano-Se⁰) under both aerobic and anaerobic conditions.
34 The biogenic nano-Se⁰ converted 45.8-57.1% and 39.1-48.6% of elemental mercury
35 (Hg⁰) in the contaminated soil to insoluble mercuric selenide (HgSe) under anaerobic
36 and aerobic conditions, respectively. Addition of sodium dodecyl sulfonate enhanced
37 Hg⁰ remediation, probably owing to the release of intracellular nano-Se⁰ from the
38 bacterial cells for Hg fixation. The reaction product after remediation was identified
39 as non-reactive HgSe that was formed by amalgamation of nano-Se⁰ and Hg⁰.
40 Biosynthesis of nano-Se⁰ both aerobically and anaerobically therefore provides a
41 versatile and cost-effective remediation approach for Hg⁰-contaminated surface and
42 subsurface soils, where the redox potential often changes dramatically.

43

44 **Keywords:** Bioremediation; selenium; mercury; metal immobilization; selenium
45 nanoparticles

46

47 **1. Introduction**

48 Mercury (Hg) is a naturally occurring non-essential highly toxic metal in the Earth's
49 crust, and it is widely used in many industries such as the extraction of gold from ores,
50 production of NaOH and chlorine in the chlor-alkali industry, and manufacture of
51 compact fluorescent lamps, cosmetics, insecticides and herbicides (Boening, 2000). In
52 some cases, improper use has led to extensive mercury pollution of soil. For example,
53 mercury concentrations in the soil around a chlor-alkali plant in the Netherlands
54 reached up to 1150 mg kg⁻¹ (Bernaus et al., 2006). Mercury emissions were also
55 detected in surrounding soils and sealed waste ponds near a chlor-alkali factory
56 (Southworth et al., 2004).

57

58 Mercury speciation in contaminated soil can be classified into water soluble,
59 elemental, exchangeable, strongly-bound, organic, sulfide and residual fractions.
60 Normally, elemental mercury comprises a small proportion of the total mercury in soil
61 whereas in mercury or gold mining regions and in chlor-alkali plant soil, elemental
62 mercury may account for a much larger part of the total mercury. In the Idrija mercury
63 mine region, Slovenia, HgS is the predominant mercury fraction, followed by Hg⁰
64 (Kocman et al., 2004). Elemental mercury accounted for ~95% of the total mercury in
65 soils heavily contaminated with mercury in Venezuela (García-Sánchez et al., 2006).
66 Soil beneath and adjacent to the Pavlodar Chemical Plant in Kazakhstan was also
67 contaminated by mercury, and ~88-98% of the total mercury can be present as
68 elemental mercury (Neculita et al., 2005). Therefore, there is an urgent need to treat

69 elemental mercury-contaminated soil, particularly that caused by the industries
70 mentioned above.

71

72 Selenium (Se) is in the same group as sulfur in the Periodic Table, and has an
73 extremely high affinity for mercury with $\Delta G^0 = -38.1 \text{ kJ mol}^{-1}$, which is higher than
74 that for sulfur (Ho et al., 2015). A large amount of work has been carried out on
75 detection of mercury and selenium in fish, marine mammals and humans. The molar
76 ratio of mercury to selenium **in such samples was** approximately 1, which suggested
77 detoxification of mercury into less toxic mercuric selenide (HgSe) (Southworth et al.,
78 2000; Squadrone et al., 2015). Selenium nanoparticles have already been shown to be
79 effective for mercury removal from off gases, and unstabilized amorphous nano-Se⁰
80 showed a strong mercury capture capacity of 188 mg g⁻¹ dry weight (Johnson et al.,
81 2008; Lee et al., 2009). Biogenic red amorphous nano-Se⁰ has also been applied to
82 sequester mercury vapour released from mercury-contaminated museum specimens,
83 the historic mercuric chloride treatment to preserve specimens leading to mercury
84 volatilization (Fellowes et al., 2011). Nano-Se⁰ therefore appears to be a promising
85 mercury-trapping agent for cleanup, disposal, recycling and packaging applications
86 (Ralston, 2008).

87

88 Most of these examples of mercury removal by selenium are concerned with mercury
89 vapour in the atmosphere. However, this technique can also be applied to the aquatic
90 environment. For example, *Pseudomonas fluorescens* could reduce SeO₃²⁻ and Hg²⁺

91 into elemental forms, the interaction between these two elements resulting in the
92 formation of Hg-Se complexes within the cells with a Hg:Se molar ratio close to 1
93 (Yang et al., 2011). Bioreduced Hg⁰ by a strain of *Shewanella putrefaciens* was
94 captured as HgSe by extracellular biogenic amorphous selenium nanospheres (Jiang et
95 al., 2012). However, no studies have been carried out which have tested the capacity
96 of biogenic nano-Se⁰ to immobilize mercury in soil.

97

98 Bioremediation of contaminated soil can be limited by the redox potential and the
99 performance of the remediating bacteria in aerobic and anaerobic conditions. Surface
100 soil layers are usually aerobic while subsurface soil layers may be anoxic, which
101 means that both aerobic and anaerobic processes may be required. In addition, the soil
102 redox potential during bioremediation may change drastically as bacterial cultures and
103 substrates are applied. This may increase the cost, complexity and performance of
104 bioremediation. Therefore, an ability for microbes to produce nano-Se⁰ both
105 aerobically and anaerobically may be relevant for the bioremediation of
106 mercury-contaminated soils. Using versatile facultative bacteria to remediate soils
107 with quite different redox potentials could be simpler and more effective.

108

109 In the present study, the performance of the facultative anaerobe *Citrobacter freundii*
110 Y9, which can produce amorphous nano-Se⁰ under anaerobic and aerobic conditions,
111 in sequestering elemental mercury in soil was evaluated. Sequential soil extraction of
112 mercury was carried out to determine changes in mercury speciation, and the reaction

113 products were characterized by scanning electron microscopy with energy-dispersive
114 X-ray spectrometry (SEM-EDS), X-ray diffraction (XRD), transmission electron
115 microscopy (TEM) and X-ray photoelectron spectroscopy (XPS).

116

117 **2. Materials and methods**

118 *2.1. Bacteriogenic nano-Se⁰*

119 *Citrobacter freundii* Y9, isolated from sludge from an anaerobic sulfate-reducing
120 bioreactor in Urumqi, China was used in this study, and the sequence has been
121 submitted to Gene Bank (number KF781347). The growth medium contained the
122 following components: 1.0 g K₂HPO₄, 0.1 g MgCl₂, 0.2% yeast extract, 10 mM
123 sodium citrate in 1 L Milli-Q water. The medium was adjusted to pH 7.0-7.2 using 0.1
124 M HCl, and sterilized in a vertical heating pressure steam (LDZX-75KBS, Shanghai,
125 China). The bacteria were cultured at 26⁰C in 500 ml serum bottles in a Whitley
126 DG250 anaerobic workstation (Don Whitley Scientific, West Yorkshire, England), and
127 aerobically in 250 ml flasks with constant shaking at 150 rpm.

128

129 To measure the selenite reduction activity of *C. freundii* Y9, late logarithmic phase
130 cells (5%) were inoculated into fresh medium containing 1 mM sodium selenite,
131 added from a sterile 500 mM sodium selenite stock solution. At appropriate time
132 intervals, samples were collected and filtered using 0.22 μm hydrophilic
133 polyestersulfone membranes. Selenite in the filtrates was analyzed by LC-HGAFS
134 (Liquid Chromatography-Hydride Generation Atomic Fluorescence Spectrometry)
135 (Jitian, Beijing, China). Determination of the number of viable cells (colony-forming
136 units, CFU) was conducted as follows to measure the growth of bacteria (Tugarova et
137 al, 2014). A series of consecutive ten-fold dilutions of bacterial suspensions were
138 made using sterile physiological saline (0.87% NaCl); 200 μl of the corresponding

139 diluted samples were then spread on solid **nutrient broth medium** and cultured for 4-5
140 d at 26⁰C. Abiotic nano-Se⁰ was prepared using L-ascorbic acid as a reductant to
141 reduce H₂SeO₃, **polyvinyl alcohol (PVA, 0.05%)** was used as a soft template. The
142 abiotic nano-Se⁰ was centrifuged at 10,000×g for 10 min and then re-suspended in
143 PVA solution (0.05%). Biogenic and abiotic selenium were characterized by
144 SEM-EDS and XRD.

145

146 *2.2. Elemental mercury immobilization in soil*

147 Biogenic and abiotic nano-Se⁰ were used to capture mercury in contaminated soil
148 under aerobic and anaerobic conditions. Soil was collected from farmland near
149 Urumqi, China, sterilized in a vertical heating pressure steam (LDZX-75KBS,
150 Shanghai, China), and air-dried, sieved (1 mm), and sterilized again under UV
151 light irradiation for 2 h. **Liquid mercury was** added to the soil directly which was then
152 aged for two months. The mercury immobilization tests were performed in centrifuge
153 tubes which contained 25 g of elemental mercury contaminated soil and 25 ml
154 medium containing 4 mM elemental selenium. When biogenic nano-Se⁰ was used to
155 treat mercury contaminated soil, one group contained 1% sodium dodecyl sulfate
156 (SDS) to lyse the bacteria and release intracellular Se⁰. The original concentration of
157 soil mercury was analyzed using a mercury analyzer (Lumex RP91C, Saint Petersburg,
158 Russia). After one week, the different mercury fractions in the soil samples were
159 analyzed. A control without addition of nano-Se⁰ was also treated in the same way.
160 The elemental selenium in the medium or in the **PVA** suspensions was centrifuged at

161 12,000×g for 10 min and then the Se-free supernatant was added to the control.
162 Anaerobic and aerobic immobilization were performed inside a Whitley DG250
163 anaerobic workstation or in a fume hood, respectively.
164
165 Sequential extraction procedures were used to evaluate mercury speciation in the soil,
166 according to previously published methods (Biester and Scholz, 1996; Shi et al.,
167 2005). Mercury compounds were classified into the following fractions: F1: total
168 mercury; F2: elemental mercury; F3: water-soluble and exchangeable mercury; F4:
169 mercury bound to organic matter; and F5: residual mercury. Total mercury (F1) was
170 analyzed using a mercury analyzer (Lumex RP91C, Saint Petersburg, Russia) and this
171 value was labelled THg1. For elemental mercury (F2), the soil was heated at 180⁰C
172 for 2 h in a muffle furnace to separate out the elemental mercury. After this treatment,
173 the total mercury left in the soil was again analyzed and this value was labelled THg2.
174 The remaining soil was set aside for the following treatment. For water-soluble
175 mercury and exchangeable mercury (F3), 20 ml Milli-Q water (18 MΩcm⁻¹) was
176 added to 2 g soil from the F2 treatment and shaken for 2 h. The mixture was then
177 centrifuged for 20 min at 12,000×g. Another 20 ml of 1 M CaCl₂ (pH=5) was added
178 to the soil and shaken for 2 h. The mixture was then centrifuged for 20 min at 12,000
179 ×g, then air dried. The total mercury left in the soil was again analyzed and this value
180 was labelled THg3. The remaining soil was set aside for the following treatment. For
181 mercury bound to organic matter (F4), 20 ml of 0.2 M NaOH was added to the treated
182 soil from F3 and shaken for 2 h. The mixture was centrifuged as described previously,

183 and then 20 ml CH₃COOH 4% (v/v) was added to the soil and shaken for 2 h. The
184 mixture was then centrifuged as previously described, air dried and the total mercury
185 left in the soil analyzed as above, which was labelled THg4. According to the
186 following formulae, the concentrations of the different mercury fractions in the soil
187 were obtained: F1= THg1; F2= THg1-THg2; F3= THg2-THg3; F4= THg3-THg4;
188 F5= THg4.

189

190 *2.3. SEM-EDS, XRD, TEM and XPS analyses*

191 The synthesized selenium particles and the soil after the experiments were analyzed
192 by SEM-EDS. These samples were first freeze-dried in a vacuum freeze dryer
193 (Labconco, Kansas, USA) then coated with gold with a sputter coater (Emitech K575,
194 Kent, UK). Samples were examined using a scanning electron microscope (Zeiss
195 Super 55VP, Oberkochen, Germany). Elemental analysis was carried out using
196 energy-dispersive X-ray spectrometry (Bruker XFlash 5010, Berlin, Germany).

197

198 Samples for XRD were first freeze-dried, and then XRD spectra were obtained using
199 an X-ray diffractometer (Bruker D8, Karlsruhe, Germany) with a Cu anode (40 kV
200 and 30 mA) and scanning from 5 to 80° 2 θ .

201

202 In order to further characterize biogenic selenium particles, TEM was conducted as
203 follows (Zhang and Frankenberger, 2006). Cells were harvested by centrifugation
204 (10,000 \times g, 10 min) and fixed with 2.5% para-formaldehyde + 2.5% glutaraldehyde

205 in 0.1 M cacodylate buffer (pH 7.2) and post-fixed with 1% OsO₄ + 0.15% ruthenium
206 red in 0.1 M cacodylate buffer. After washing three times with Milli-Q water, cells
207 were dehydrated in graded acetone solutions (30, 50, 70, 90 and 100% for 15 min
208 each time) and then embedded in Epon-Araldite. Blocks were sectioned using a
209 Reichert Supernova Microtome (Leica AG, Wien, Austria) using a diamond knife
210 producing sections approximately 80 nm in thickness. The samples were observed
211 using a JEM-1200EX electron microscope (JEOL, Tokyo, Japan).

212

213 X-ray photoelectron spectroscopy was carried out on powders using a Thermo
214 ESCALAB 250Xi spectrometer (Thermo Fisher Scientific, Waltham, MA, USA)
215 using an Al Ka monochromatized source. Surface charging effects were corrected
216 with a C 1s peak at 284.6 eV as a reference. Curve fitting and decomposition were
217 achieved assuming Gaussian-Lorentzian fitting following Shirley background
218 subtraction.

219

220 *2.4. Reagents*

221 All the chemicals and reagents used in this study were of analytical grade. **SDS**,
222 H₂SeO₃ and Na₂SeO₃ were supplied by Guang Fu (Tianjin, China). Selenite was
223 prepared as a 500 mM stock solution in Milli-Q water (18 MΩcm⁻¹) and sterilized
224 using 0.22 μm hydrophilic polyestersulfone membrane filters (Shanghai, China).
225 Liquid mercury was obtained from Sinopharm Chemical Reagent (Shanghai, China).
226 **PVA** was obtained from Sigma-Aldrich Ltd. L-ascorbic acid was supplied by Yong

227 Sheng (Tianjin, China).

228

229 *2.5. Statistical analysis*

230 The size of selenium particles was calculated using Image-Pro Plus 6.0 based on SEM

231 spectra. All experiments were carried out in triplicate; error bars on figures show

232 standard deviations'.

233

234 **3. Results and discussion**

235 *3.1. Bacteriogenic nano-Se⁰*

236 *C. freundii* Y9 could reduce selenite to elemental selenium particles, which was
237 evident by the colour of the medium changing to red/orange, under both aerobic and
238 anaerobic treatments. There was no colour change and no change of selenite
239 concentration in the abiotic control which demonstrated that it was the presence of
240 growing bacteria that led to the reduction of selenite. After inoculation, bacterial
241 growth was concomitant with the process of reduction. *C. freundii* Y9 showed more
242 tolerance to selenite under anaerobic conditions and over 24 h, the medium turned red,
243 and there was a rapid decrease in selenite concentration with complete removal after 5
244 d (Fig. 1). However, under aerobic conditions the medium turned a weaker red after
245 24 h with the efficiency of selenite reduction being 27% after 5 d incubation, the
246 concentration of selenite remaining stable after this time (Fig. 1). Anaerobic selenite
247 reduction was rapid and more pronounced than in aerobic conditions. In an anaerobic
248 mode of respiration, selenite can be used as an electron acceptor in dissimilatory
249 reduction (Macy et al., 1989), or be reduced and incorporated into organic compounds
250 in assimilatory reduction (Lortie et al., 1992; Gadd, 1993). However, the mechanisms
251 under aerobic conditions are not clearly understood.

252

253 **SEM** of *C. freundii* Y9 showed that particles were present inside the cells after
254 exposure to 1 mM selenite; such particles were also detected extracellularly (Fig. 2b, c,
255 d). **EDS** spectra of the particles confirmed the presence of selenium with characteristic

256 selenium absorption peaks at 1.37 and 11.22 keV (Fig. 2e). The calculated diameter of
257 selenium particles ranged from 200-800 nm, with the average diameter being $580 \pm$
258 109 nm. XRD patterns showed a broad peak at 2θ values from 25° to 30° , which
259 indicated that the selenium particles formed were amorphous in nature (Fig. 2f). TEM
260 showed that electron-dense particles were present inside the cells near the cytoplasmic
261 membrane after incubation with 1 mM selenite (Fig. 2g, h). The biogenic selenium
262 was deposited inside the cells or extracellularly and during cell lysis the elemental
263 selenium could be released into the extracellular medium.

264

265 *C. freundii* is commonly found in soil, freshwater and marine habitats. Although,
266 selenate reduction has been reported in *C. freundii* (Zhang et al., 2008), there is less
267 work on selenite reduction, and the electron transfer system is different between
268 selenate and selenite reduction in this organism (Siddique et al., 2006). As selenate is
269 generally more toxic than selenite (Hockin and Gadd, 2003, 2006), it is perhaps better
270 to use selenite as an electron acceptor to obtain nano- Se^0 .

271

272 3.2. Abiotic nano- Se^0

273 The mixture of PVA-stabilized selenium nanoparticles had a red/orange colour and
274 remained stable on prolonged incubation. SEM and EDS spectra confirmed the
275 presence of elemental nano- Se^0 (Fig. 3). The diameters of these nano- Se^0 particles
276 ranged from 10-90 nm with an average value of 71 ± 16 nm. However, without PVA in
277 solution, a dark red precipitate of Se^0 appeared. The XRD pattern of

278 chemically-reduced elemental selenium was the same as that for biogenic elemental
279 selenium, indicating that the elemental selenium formed here was also amorphous.

280

281 *3.3. Elemental mercury immobilization in soil*

282 The ability of biogenic and abiotic elemental amorphous nano-Se⁰ to immobilize Hg⁰
283 in soil was comparatively studied. The total mercury in the contaminated soil was
284 $21.43 \pm 2.51 \mu\text{g g dry weight}^{-1}$ which is ~350-fold higher than values commonly
285 found. Elemental mercury was the primary fraction ($17.63 \pm 2.10 \mu\text{g g}^{-1}$ dry weight)
286 which accounted for 78.2-84.6% of the total mercury, while 11.1-11.7% (2.46 ± 0.28
287 $\mu\text{g g}^{-1}$) of the mercury occurred in the insoluble residual mercury fraction. When
288 mercury-contaminated soil was supplied with nano-Se⁰, the total mercury decreased
289 only slightly, some possibly being volatilized or adhering to surfaces of the bioreactor.
290 However, the mercury speciation changed significantly, especially in the elemental
291 and residual fractions (Fig. 4). Under anaerobic conditions, Hg⁰ present in the
292 mercury-contaminated control decreased by 11.3% ($1.99 \mu\text{g g}^{-1}$). However, there was
293 a 73.5% ($12.96 \mu\text{g g}^{-1}$) and 63.5% ($11.20 \mu\text{g g}^{-1}$) decrease in Hg⁰ when the soil was
294 supplied with biogenic Se⁰ + SDS and biogenic Se⁰, respectively. The SDS was used
295 in an attempt to release intracellular Se⁰ from the bacterial cells and therefore enhance
296 the reaction between Hg⁰ and Se⁰. For the abiotic Se⁰ treatment, 49.2% ($8.68 \mu\text{g g}^{-1}$)
297 of the Hg⁰ fraction decreased. Under aerobic conditions, Hg⁰ present in the control
298 decreased by 12.5% ($2.67 \mu\text{g g}^{-1}$). However, there was a 65.8% ($11.60 \mu\text{g g}^{-1}$) and
299 61.25% ($10.79 \mu\text{g g}^{-1}$) decrease in Hg⁰ when the soil was supplied with biogenic Se⁰ +

300 SDS and biogenic Se^0 , respectively. For the abiotic aerobic Se^0 treatment, Hg^0
301 decreased by 38.9% ($6.87 \mu\text{g g}^{-1}$). Concomitant with the decrease in Hg^0 , the residual
302 mercury fraction was found to increase significantly. Under anaerobic conditions,
303 residual mercury in the mercury-contaminated control increased by $0.73 \mu\text{g g}^{-1}$.
304 However, there was a $10.79 \mu\text{g g}^{-1}$ and $8.80 \mu\text{g g}^{-1}$ increase in residual mercury when
305 the soil was supplied with biogenic $\text{Se}^0 + \text{SDS}$ and biogenic Se^0 , respectively. For the
306 abiotic Se^0 treatment, residual mercury increased by $4.44 \mu\text{g g}^{-1}$. Under aerobic
307 conditions, residual mercury in the control increased by $0.85 \mu\text{g g}^{-1}$. However, there
308 was a $9.41 \mu\text{g g}^{-1}$ and $7.75 \mu\text{g g}^{-1}$ increase in residual mercury when the soil was
309 supplied with biogenic $\text{Se}^0 + \text{SDS}$ and biogenic Se^0 , respectively. For the abiotic
310 aerobic Se^0 treatment, residual mercury was increased by $3.15 \mu\text{g g}^{-1}$. Thus, addition
311 of abiotic or bacterially-produced **nano- Se^0** to mercury-contaminated soil under
312 anaerobic and aerobic conditions led to a decrease in the proportion of Hg^0 present,
313 and an increase in the insoluble residual Hg fraction.

314

315 The efficiency of abiotic **nano- Se^0** preparations was less than that for biogenic
316 **nano- Se^0** after SDS treatment which is surprising since the diameter of the abiotic
317 **nano- Se^0** (10-90 nm) was much smaller than that of biogenic **nano- Se^0** (200-800 nm).
318 In general terms, selenium capture of mercury occurs by a gas-solid reaction where
319 the capacities and kinetics mainly depend on surface area: smaller particles have a
320 larger specific surface area (Johnson et al., 2008). However, the **PVA** template may
321 have blocked some elemental mercury access to elemental selenium which would

322 inhibit the reaction between selenium and mercury. Other workers have found similar
323 results, e.g. BSA-stabilized nano-Se⁰ had a lower sorption capacity than conventional
324 selenium powder despite a much smaller particle size (6-60 nm vs 10-200 μm)
325 (Johnson et al., 2008). Thus, biogenic nano-Se⁰ gave a better performance for Hg⁰
326 immobilization in soil.

327

328 *3.4 Speciation of Hg immobilized in soil*

329 According to the SEM-EDS of immobilization products (Fig. 5), the atomic ratio of
330 Hg:Se is close to 1 (Table 1), which revealed the formation of HgSe. XRD (Fig. 6)
331 also confirmed that mercury and selenium were in the form of HgSe (PDF#65-2892).
332 XPS analysis shows that binding energy of Hg 4f_{7/2} and Hg 4f_{5/2} was observed at 99.2
333 eV and 104.3 eV, respectively (Fig. 7), indicating that mercury could be present as
334 HgSe and HgO (Zylberajch-Antoine et al., 1991). Deconvolution of the high
335 resolution XPS spectra of selenium shows the presence of binding energy peaks of Se
336 3d_{5/2} at 53.8 eV and Se 3d_{3/2} at 54.5 eV, which is in good agreement with that
337 previously reported for HgSe (Wall et al., 1986). The binding energy values for Se⁰ at
338 Se 3d_{5/2} (54.7 eV) and Se 3d_{3/2} (55.2 eV) were in accordance with those reported in
339 the literature (Miyake et al., 1984). The XPS results confirmed immobilization of Hg⁰
340 by nano-Se⁰ as HgSe.

341

342 To date, many technologies have been examined for remediation of
343 mercury-contaminated soil, such as immobilization (stabilization or solidification)

344 electro-remediation, soil flushing and soil washing, vitrification, thermal desorption
345 and phytoremediation (Wang et al., 2012). Thermal treatment is the most widely used
346 method although the treated soil is unsuitable for reuse due to the destruction of
347 original soil properties (Yang et al., 2008), with some techniques also leading to
348 mercury release into the air (Wang et al., 2012). The work presented here has shown
349 that **amorphous nano-Se⁰** is capable of capturing Hg⁰ in both surface and subsurface
350 soil, thereby reducing mobility due to the production of HgSe. HgS is the typical
351 residual form of mercury in soil, but HgSe also has a very low solubility ($K_{sp}=10^{-58}$)
352 and is more stable than HgS (Björnberg et al., 1988). As well as this, the use of
353 nano-Se⁰ appears safer since HgSe is chemically inert and a much less toxic
354 compound compared to other forms of mercury and selenium. In addition, nano-Se⁰ is
355 unharmed, and the median lethal dose (LD50) for nano-Se⁰ is 6.7 g kg⁻¹ in rats
356 (Cummins and Kimura, 1971). Therefore, immobilization of mercury with nano-Se⁰
357 may provide an efficient means of soil remediation with no secondary pollution and
358 no volatilization. **However, soil is a heterogeneous complex environment, and it is**
359 **necessary to consider the wider applicability of this technique across different soil**
360 **types and physico-chemical conditions as well as the stability of nano-Se⁰. Moreover,**
361 **the effects of different soil compositions and conditions on the reaction between**
362 **nano-Se⁰ and Hg⁰ also need to be taken into consideration.**

363

364 **4. Conclusions**

365 This work is the first demonstration that **amorphous nano-Se⁰** can be applied to

366 capture Hg⁰ in soil under both aerobic and anaerobic conditions. It is concluded that *C.*
367 *freundii* could be more easily and successfully applied for remediation of surface and
368 subsurface soils, where the redox potential often changes dramatically. The
369 experiments have revealed the formation of non-reactive HgSe by amalgamation of
370 elemental selenium and elemental mercury which provides a potential approach for
371 mercury immobilization in mercury-contaminated sites.

372

373 **Conflict of Interest**

374 The authors declare that they have no conflict of interest.

375

376 **Acknowledgements**

377 This work was supported by the National Natural Science Foundation of China
378 (U1120302 and 21177127). G. M. Gadd gratefully acknowledges receipt of an award
379 under the Chinese Government's 1000 Talents Plan with the Xinjiang Institute of
380 Ecology and Geography, Chinese Academy of Sciences, Urumqi, China. G. M. Gadd
381 also gratefully acknowledges an award (NE/M01090/1) under the National
382 Environmental Research Council (UK) Security of Supply of Mineral Resources
383 Grant Program: Tellurium and Selenium Cycling and Supply (TeASe). Partial funding
384 for this research was also received from the Visiting Professor Program at King Saud
385 University, Riyadh, Saudi Arabia.

386

387 **References:**

- 388 Bernaus, A., Gaona, X., Derk, V.R., Valiente, M., 2006. Determination of mercury in
389 polluted soils surrounding a chlor-alkali plant: direct speciation by X-ray absorption
390 spectroscopy techniques and preliminary geochemical characterisation of the area.
391 *Anal. Chim. Acta* 565, 73-80.
- 392 Biester, H., Scholz, C., 1996. Determination of mercury binding forms in
393 contaminated soils: mercury pyrolysis versus sequential extractions. *Environ. Sci.*
394 *Technol.* 31, 233-239.
- 395 Björnberg, A., Håkanson, L., Lundbergh, K., 1988. A theory on the mechanisms
396 regulating the bioavailability of mercury in natural waters. *Environ. Pollut.* 49, 53-61.
- 397 Cummins, L.M., Kimura, E.T., 1971. Safety evaluation of selenium sulfide
398 anti-dandruff shampoos. *Toxicol. Appl. Pharmacol.* 20, 89-96.
- 399 Boening, D.W., 2000. Ecological effects, transport, and fate of mercury: a general
400 review. *Chemosphere* 40, 1335-1351.
- 401 Fellowes, J.W., Patrick, R.A., Green, D.I., Dent, A., Lloyd, J.R., Pearce, C.I., 2011.
402 Use of biogenic and abiotic elemental selenium nanospheres to sequester elemental
403 mercury released from mercury contaminated museum specimens. *J. Hazard. Mater.*
404 189, 660-669.
- 405 Gadd, G.M., 1993. Microbial formation and transformation of organometallic and
406 organometalloid compounds. *FEMS Microbiol. Rev.* 11, 297-316.
- 407 García-Sánchez, A., Contreras, F., Adams, M., Santos, F., 2006. Atmospheric mercury
408 emissions from polluted gold mining areas (Venezuela). *Environ. Geochem. Health* 28,

409 529-540.

410 Ho, C.T., Nguyen, A.T., Duong, T.T., Dang, D.K., Tang, T.C., Hur, H.G., 2015.

411 Biologically based method for the synthesis of Hg–Se nanostructures by *Shewanella*

412 spp. RSC Adv. 5, 20764-20768.

413 Hockin, S.L., Gadd, G.M., 2003. Linked redox precipitation of sulfur and selenium

414 under anaerobic conditions by sulfate-reducing bacterial biofilms. Appl. Environ.

415 Microbiol. 69, 7063-7072.

416 Hockin, S., Gadd, G.M., 2006. Removal of selenate from sulfate-containing media by

417 sulfate-reducing bacterial biofilms. Environ. Microbiol. 8, 816-826.

418 Jiang, S., Ho, C.T., Lee, J.H., Duong, H.V., Han, S., Hur, H.G., 2012. Mercury capture

419 into biogenic amorphous selenium nanospheres produced by mercury resistant

420 *Shewanella putrefaciens* 200. Chemosphere 87, 621-624.

421 Johnson, N.C., Manchester, S., Sarin, L., Gao, Y., Kulaots, I., Hurt, R.H., 2008.

422 Mercury vapor release from broken compact fluorescent lamps and in situ capture by

423 new nanomaterial sorbents. Environ. Sci. Technol. 42, 5772-5778.

424 Kocman, D., Horvat, M., Kotnik, J., 2004. Mercury fractionation in contaminated

425 soils from the Idrija mercury mine region. J. Environ. Monit. 6, 696-703.

426 Lee, B., Sarin, L., Johnson, N.C., Hurt, R.H., 2009. A nano-selenium reactive barrier

427 approach for managing mercury over the life-cycle of compact fluorescent lamps.

428 Environ. Sci. Technol. 43, 5915-5920.

429 Lortie, L., Gould, W.D., Rajan, S., McCready, R.G.L., Cheng, K.J., 1992. Reduction

430 of selenate and selenite to elemental selenium by a *Pseudomonas stutzeri* isolate. Appl.

431 Environ. Microbiol. 58, 4042-4044.

432 Macy, J.M., Michel, T.A., Kirsch, D.G., 1989. Selenate reduction by a *Pseudomonas*
433 species: a new mode of anaerobic respiration. FEMS Microbiol. Lett. 61, 195-198.

434 Miyake, I., Tanpo, T., Tatsuyama, C., 1984. XPS study on the oxidation of InSe. Jpn. J.
435 Appl. Phys. 23, 172.

436 Neculita, C.M., Zagury, G.J., Deschênes, L., 2005. Mercury speciation in highly
437 contaminated soils from chlor-alkali plants using chemical extractions. J. Environ.
438 Qual. 34, 255-262.

439 Ralston, N. Nano-selenium captures mercury. Nat. Nanotechnol. 2008; 3: 648.

440 Shi, J., Liang, L., Jiang, G., Jin, X., 2005. The speciation and bioavailability of
441 mercury in sediments of Haihe River, China. Environ. Int. 31, 357-365.

442 Siddique, T., Zhang, Y., Okeke, B.C., Frankenberger, W.T., 2006. Characterization of
443 sediment bacteria involved in selenium reduction. Bioresour. Technol. 97,1041-1049.

444 Southworth, G.R., Lindberg, S.E., Zhang, H., Anscombe, F.R., 2004. Fugitive mercury
445 emissions from a chlor-alkali factory: sources and fluxes to the atmosphere. Atmos.
446 Environ. 38, 597-611.

447 Southworth, G.R., Peterson, M.J., Ryon, M.G., 2000. Long-term increased
448 bioaccumulation of mercury in largemouth bass follows reduction of waterborne
449 selenium. Chemosphere 41, 1101-1105.

450 Squadrone, S., Benedetto, A., Brizio, P., Prearo, M., Abete, M.C., 2015. Mercury and
451 selenium in European catfish (*Silurus glanis*) from Northern Italian Rivers: Can molar
452 ratio be a predictive factor for mercury toxicity in a top predator? Chemosphere 119,

453 24-30.

454 Tugarova, A.V., Vetchinkina, E.P., Loshchinina, E.A., Burov, A.M., Nikitina, V.E.,
455 Kamnev, A.A., 2014. Reduction of selenite by *Azospirillum brasilense* with the
456 formation of selenium nanoparticles. *Microb. Ecol.* 68, 495-503.

457 Wall, A., Caprile, C., Franciosi, A., Vaziri, M., Reifenberger, R., Furdyna, J., 1986.
458 Bonding and stability in narrow-gap ternary semiconductors for infrared applications.
459 *J. Vac. Sci. Technol. A* 4, 2010-2013.

460 Wang, J., Feng, X., Anderson, C.W., Xing, Y., Shang, L., 2012. Remediation of
461 mercury contaminated sites – a review. *J. Hazard. Mater.* 221, 1-18.

462 Yang, D., Chen, Y., Belzile, N., 2011. Evidences of non-reactive mercury-selenium
463 compounds generated from cultures of *Pseudomonas fluorescens*. *Sci. Total Environ.*
464 409, 1697-1703.

465 Yang, D., Chen, Y., Gunn, J.M., Belzile, N., 2008. Selenium and mercury in
466 organisms: interactions and mechanisms. *Environ. Rev.* 16, 71-92.

467 Zhang, Y., Frankenberger, W.T., 2006. Removal of selenite in river and drainage
468 waters by *Citrobacter braakii* enhanced with zero-valent iron. *J. Agric. Food Chem.*
469 54, 152-156.

470 Zhang, Y., Okeke, B.C., Frankenberger, W.T., 2008. Bacterial reduction of selenate to
471 elemental selenium utilizing molasses as a carbon source. *Bioresour. Technol.* 99,
472 1267-1273.

473 Zylberajch-Antoine, C., Barraud, A., Roulet, H., Dufour, G., 1991. XPS
474 characterization of inserted mercury sulfide single layers in a Langmuir-Blodgett

475 matrix. Appl. Surf. Sci. 52, 323-327.

476

477 **Table 1.** The atom concentrations of selenium, mercury and the atomic ratio between
 478 selenium and mercury in mercury-contaminated soil after addition of elemental
 479 selenium.

	1	2	3	4	5	6	7	8
Atom.C: Hg [at.%]	24.11	19.63	26.09	21.53	24.62	25.89	25.51	28.02
Atom.C: Se [at.%]	21.99	22.02	23.87	20.52	22.15	23.98	22.59	23.8
Atomic ratio Hg/Se	1.096	0.891	1.093	1.049	1.111	1.080	1.129	1.177

480 As shown in Fig. 5(a), eight points were selected for EDS, and the concentrations of
 481 selenium, mercury and the atomic ratio between selenium and mercury were
 482 calculated according to the EDS results.

483

484 **Figure legends**

485 **Fig. 1.** Growth and reduction kinetics at an initial concentration of 1 mM Na₂SeO₃.

486 Symbols represent: (■) selenite concentration under anaerobic conditions; (□) selenite

487 concentration under aerobic conditions; (▼) CFU under a

488 CFU under aerobic conditions. Error bars (n=3) represent the standard deviation.

489

490 **Fig. 2.** Characterization of elemental selenium produced by *C. freundii* Y9. (a) SEM

491 micrographs of *C. freundii* Y9. (b, c, d) SEM micrographs of *C. freundii* Y9 grown in

492 the presence of 1 mM selenite for 5 d. (e) EDS spectrum and (f) XRD pattern of red

493 selenium particles produced by *C. freundii* Y9 grown in the presence of 1 mM selenite

494 for 5 d. (g, h) Transmission electron micrographs of the cells cultured in 1 mM

495 selenite for 5 d. Scale bars: (a, b) 1 μm; (c, d, g, h) 200 nm. Typical results are shown

496 from one of several determinations.


497

498 **Fig. 3.** SEM micrograph of abiotic elemental selenium. Scale bars = 1 μm. A typical

499 micrograph is shown from one of several determinations.

500

501 **Fig. 4.** Different fractions of mercury in soil before and after experimental treatments.

502 (a) anaerobic conditions. (b) aerobic conditions. Symbols represent:  total

503 mercury;  elemental mercury;  water soluble and exchangeable mercury;

504  mercury bound to organic matter;  residual mercury. Error bars (n=3)

505 represent the standard deviations.

506 **Fig. 5.** SEM-EDS micrograph of mercury contaminated soil after addition of
507 elemental selenium. (a) SEM micrograph (scale bar = 2 μm) and (b) EDS spectrum of
508 mercury contaminated soil after addition of elemental selenium. Typical results are
509 shown from one of several determinations.

510

511 **Fig. 6.** XRD pattern of mercury contaminated soil after addition of elemental
512 selenium. (a) XRD pattern of mercury contaminated soil. (b) XRD pattern of mercury
513 contaminated soil with addition of elemental selenium. A typical pattern is shown
514 from one of two determinations both of which gave similar results.

515

516 **Fig.7.** High resolution XPS spectrum. (a) XPS spectroscopy of Hg 4f in experimental
517 soil; (b) XPS spectroscopy of Se 3d in experimental soil. Symbols represent:
518 experimental spectrum; — interpolate spectrum; — fitted peaks; — loss feature;
519 — background.